

**INFLUENCE OF TRANSVERSE ELEMENTS ON THE
PULLOUT CAPACITY OF METAL STRIP REINFORCEMENT
IN SANDY SOIL**

By

JAVAD ESFANDIARI

**Thesis submitted in fulfilment of the requirements
for the degree of
Doctor of Philosophy**

2014

DECLARATIONS

I declare that this thesis is the results of my own research, that is does not incorporate without acknowledgment any material submitted for a degree or diploma in any university and does not contain any material previously published, written or produced by another person except where due reference is made in the text.

Signed: _____

Candidate's name: Javad Esfandiari

Date:

Signed: _____

Supervisor's name: Prof. Dr. Mohammad Razip Selamat

Date:

ACKNOWLEDGEMENTS

All praises are due to the Creator who reigns over all creations. This thesis is the results of years of work whereby I have been accompanied and supported by many people. It is a pleasant aspect that I have now the opportunity to express my gratitude to all of them.

First and foremost, I would like to express my deepest appreciation to my supervisor Prof. Dr. Mohammad Razip Selamat for the supervision, technical guidance, encouragement, and constant dedication throughout the duration of this research. I owe him a lot of gratitude for having me shown the path of this research. I have learned so many new things from him. Besides being an excellent supervisor, Prof. Dr. Mohammad Razip Selamat was more like a close relative or a good friend to me. I would also like to thank my father and my mother for their prayer and supports. I owe my loving thanks to my wife Sara Esfandiari for supporting me when she has lost a lot due to my research work. Without her encouragement and understanding of me being abroad it would have been impossible for me to finish this research.

During this research I have been helped by many people such as the technicians of geotechnical engineering laboratory Mr. Dziauddin Zainol Abidin and Mr. Muhamad Zabidi Yusuff; of concrete laboratory Mr. Abdullah Md Nanyan and Mr. Mohd. Fouzi Ali; of the School of Mechanical Engineering Mr Baharom Awang, Mohd Sani Sulaiman, and Mohd Shawal Faizal Ismail; and of the School of Material and Mineral Resources Engineering - I wish to extend my warmest thanks to all of them.

TABLE OF CONTENTS

| | |
|-------------------|------|
| DECLARATIONS | II |
| ACKNOELEDGEMENT | III |
| TABLE OF CONTENTS | IV |
| LIST OF TABLES | X |
| LIST OF FIGURES | XII |
| LIST OF SIMBOLS | XXXI |
| ABSTRAK | XXLI |
| ABSTRACT | XXXI |

| | |
|---|-----------|
| CHAPTER 1 INTRODUCTION | 1 |
| 1.1 Introduction | 1 |
| 1.2 Applications in Malaysia and abroad | 4 |
| 1.3 Recent trends in the use of geosynthetic | 6 |
| 1.4 Problem Statement | 7 |
| 1.5 Objectives of the research | 8 |
| 1.6 Scope of Research | 9 |
| 1.7 Structure of Thesis | 10 |
| | |
| CHAPTER 2: LITERATURE REVIEWS | 11 |
| 2. 1 Introduction | 11 |
| 2. 2 Pull out and direct shear tests involving reinforcement material | 11 |
| 2. 3 Effects of boundary conditions | 30 |
| 2. 4 Standards for pull out box dimensions | 33 |
| 2. 5 Finite Element Modelling (FEM) | 36 |
| 2. 6 Theoretical studies (Sawicki, A. (2000)) | 43 |
| 2. 7 Pull out mechanisms of reinforcement (Sawicki, A. (2000)) | 48 |
| 2. 8 Different pull out capacity equations by other researchers | 51 |
| 2. 9 Application of Buckingham π theorem in reinforced soil | 55 |

| | |
|--|-----------|
| 2. 10 Summary | 56 |
| CHAPTER 3: MATERIALS AND METHODS | 58 |
| 3. 1 Introduction | 58 |
| 3. 2 Materials for pull out tests | 58 |
| 3.2. 1.Strips | 60 |
| 3.2. 2 Longitudinal member | 60 |
| 3.2. 3 Ribs in place of anchorage elements | 63 |
| 3.2. 4 Anchorage elements in place of ribs | 63 |
| 3.2. 5 Stiffeners | 65 |
| 3.2. 6 Welding work | 66 |
| 3.2. 7 Galvanized coating on strips. | 69 |
| 3. 3 Materials for direct shear tests | 72 |
| 3. 4 Soil used in this study | 72 |
| 3. 5 Experimental programs | 77 |
| 3.5. 1 Compaction test | 79 |
| 3.5.2 Tensile tests | 81 |
| 3.5.3 Triaxial test | 85 |
| 3.5.4 Pull out test | 89 |
| 3.5.5 Direct shear test | 98 |
| 3. 6 Finite Element modelling with Plaxis software | 100 |
| 3. 7 Conclusion | 101 |

| | |
|---|-----|
| CHAPTER 4 : RESULTS AND DISCUSSIONS | 104 |
| 4. 1 Tensile tests | 104 |
| 4. 2 Pullout test program I | 108 |
| 4.2. 1 Pullout Test on Plain Strip with $\sigma_n= 50$ kPa, 75 kPa, and 100 kPa | 110 |
| 4.2. 2 Pullout Test on ribbed Strip on one side with $\sigma_n=50$ kPa, 75 kPa, and 100 kPa | 114 |
| 4.2. 3 Pullout Test on ribbed Strip on both sides with $\sigma_n=50$ kPa, 75 kPa, and 100 kPa | 118 |
| 4.2. 4 Pullout Test on Strip with one anchorage element which height was 2 cm and $\sigma_n=50$ kPa, 75 kPa, and 100 kPa | 122 |
| 4.2. 5 Increase in strip-soil angle of friction with changing strip type | 127 |
| 4.2. 6 Pullout Test on Strip with one anchorage element which depth was 4 cm and $\sigma_n=50$ kPa, 75 kPa, and 100 kPa | 128 |
| 4.2. 7 Pullout Test on Strip with one anchorage element which depth was 6 cm and $\sigma_n=50$ kPa, 75 kPa, and 100 kPa | 131 |
| 4.2. 8 Pullout Test on Strip with one anchorage element which depth was 8 cm and $\sigma_n=50$ kPa, 75 kPa, and 100 kPa | 136 |
| 4.2. 9 Increase in equivalent strip-soil angle of friction with changing strip | 140 |
| 4. 3 Pullout test program II | 142 |
| 4.3. 1 Pullout Test on Strip with 2 anchorage elements ($n=2$) which depth was 2 cm ($h=2$ cm depth) and $\sigma_n=50$ kPa, 75 kPa, and 100 | 146 |
| 4.3. 2 Pullout Test on Strip with 2 anchorage elements ($n=2$) which depth was 4 cm ($h=4$ cm) and $\sigma_n=50$ kPa, 75 kPa, and 100 kPa | 150 |
| 4.3. 3 Pullout Test on Strip with 2 anchorage elements ($n=2$) which depth was 6 cm ($h=6$ cm) and $\sigma_n=50$ kPa, 75 kPa, and 100 kPa | 154 |
| 4.3. 4 Pullout Test on Strip with 2 anchorage elements ($n=2$) which depth was 8 cm ($h=8$ cm) and $\sigma_n=50$ kPa, 75 kPa, and 100 kPa | 158 |
| 4.3. 5 Pullout Test on Strip with 3 anchorage elements ($n=3$) which depth was 2 cm ($h=2$ cm) and $\sigma_n=50$ kPa, 75 kPa, and 100 kPa | 164 |
| 4.3. 6 Pullout Test on Strip with 3 anchorage elements ($n=3$) which depth was 4 cm ($h=4$ cm) and $\sigma_n=of 50$ kPa, 75 kPa, and 100 kPa | 184 |
| 4.3. 7 Pullout Test on Strip with 3 anchorage elements ($n=3$) which depth was 6 cm ($h=6$ cm) and $\sigma_n=50$ kPa, 75 kPa, and 100 kPa | 171 |
| 4.3. 8 Pullout Test on Strip with 3 anchorage elements ($n=3$) which depth was 8 cm ($h=8$ cm) and $\sigma_n=50$ kPa,, 75 kPa, and 100 kPa | 175 |

| | |
|--|-----|
| 4.3. 9 Pullout Test on Strip with 4 anchorage elements (n=4) which depth was 2 cm (h=2 cm) and $\sigma_n=50$ kPa, 75 kPa, and 100 kPa | 180 |
| 4.3. 10 Pullout Test on Strip with 4 anchorage elements (n=4) which depth was 4 cm (h=4 cm) and $\sigma_n=50$ kPa, 75 kPa, and 100 kPa | 184 |
| 4.3. 11 Pullout Test on Strip with 4 anchorage elements (n=4) which depth was 6 cm (h=6 cm) and $\sigma_n=50$ kPa, 75 kPa, and 100 kPa | 188 |
| 4.3. 12 Pullout Test on Strip with 4 anchorage elements (n=4) which depth was 8 cm (h=8 cm) and $\sigma_n=50$ kPa, 75 kPa, and 100 kPa | 192 |
| 4.3. 13 Summary of results from pull out tests involving strips of various counts of anchorage element and of various depths | 197 |
| | |
| 4. 4. Pullout test program III | 199 |
| | |
| 4.4. 1 Pullout Test on Strip with both sides having 1 anchorage element each (n=2), of 2,4, 6 and 8cm (h=2, 4, 6, 8 cm) depth, and $\sigma_n=50$ kPa, | 202 |
| 4.4. 2 Pullout Test on Strip with both sides having 4 anchorage elements each (n=8), of 2, 4, 6, and 8 cm (h=2,4,6,8 cm) depth, and $\sigma_n=100$ kPa | 208 |
| 4.4. 3 Pullout Test on Strip with both sides having 2 anchorage elements each (n=4), of 6 cm (h=6 cm) depth, and $\sigma_n=100$ kPa. | 212 |
| 4. 5 Summary of performance of strips with main geometries | 213 |
| | |
| 4.5. 1 Effect of depth of elements versus pull out capacity | 213 |
| 4.5. 2 Effect of count of elements versus pull out capacity | 217 |
| 4.5. 3 Design graphs for practical study in field | 221 |
| | |
| 4. 6 Test program IV | 223 |
| | |
| 4.6. 1 Results from direct shear tests | 223 |
| | |
| 4. 7 Regression analysis on Pullout Tests | 229 |
| | |
| 4. 8 Results of Finite Element Modelling | 236 |
| | |
| 4.8. 1 Finite element modelling of pullout test on plain strip. | 237 |
| 4.8. 2 Finite element modelling of pullout tests on strips with one anchorage element with depths ranging from 2 cm to 8 | 240 |
| 4.8. 3 Finite element modelling of pullout tests on strips with two anchorage elements with depths ranging from 2 cm to 8 cm | 251 |

| | |
|---|-----|
| 4.8. 4 Finite element modelling of pullout tests on strips with three anchorage elements with depths ranging from 2 cm to 8 cm | 260 |
| 4.8. 5 Finite element modelling of pullout tests on strips with four anchorage elements with depths ranging from 2 cm to 8 cm | 270 |
| 4.8. 6 . Summary of finite element modelling of pullout tests on strips with none, 1, 2, 3, and 4 anchorage elements, and with depths ranging from 2 cm to 8 cm | 280 |
| CHAPTER 5 : CONCLUSIONS AND RECOMMENDATIONS | 289 |
| 5. 1. Conclusions | 289 |
| 5. 2. Suggestion for Future Works | 291 |
| REFERENCES | 292 |
| LIST OF PUBLICATION | 305 |

LIST OF TABLES

| | |
|---|-----|
| Table 3. 1: Geometry specifications of strips designed for pull out tests | 61 |
| Table 3. 2: Minimum required leg length for fillet welding (LANL, 2006) | 69 |
| Table 3. 2: Minimum required leg length for fillet welding (LANL, 2006) | 71 |
| Table 3. 4: Geometry specifications of plates designed for direct shear tests | 74 |
| Table 3. 5. Summary of properties of soil used in the study | 78 |
| Table 3. 6: A summary of work carried out in this study | 102 |
| Table 4. 1: Results of tensile tests on plain strip | 105 |
| Table 4. 2: Pull out test program I | 109 |
| Table 4. 3: Pull out test program II | 143 |
| Table 4. 4: Pull out test program III | 201 |
| Table 4. 5: Pull out test program IV | 224 |
| Table 4. 6. A summary of results from direct shear tests | 227 |
| Table 4. 7: Modelling data: (a) Summary of model, (b) Coefficients (a) and ANOVA (b), and (c) Coefficients of dimensionless parameter | 230 |
| Table 4. 8: Results from various pull out tests and related dimensionless parameters | 231 |
| Table 4. 9: Parameters and results from validation tests | 233 |

| | |
|---|-----|
| Table 4. 10: Specifications and results of pull out tests on strips with elements | 234 |
| Table 4. 11: Summary of finite element modelling on plain strip | 240 |
| Table 4. 12: Summary of modelling strips with one anchorage element | 250 |
| Table 4. 13: Summary of modelling strips with two anchorage elements | 260 |
| Table 4. 14: Summary of modelling strips with three anchorage elements | 269 |
| Table 4. 15: Summary of modelling strips with four anchorage element | 279 |

LIST OF FIGURES

| | |
|--|----------|
| Figure 1. 1: A profile of commonly installed mechanically reinforced earth | 4 |
| Figure 1. 2: A view of MSE from the front showing decorative facing | 5 |
| Figure 2. 1: Results from pullout test using geogrid and lightweight aggregate (Bakeer et al., 1998b) | 16 |
| Figure 2.2: Results from interface test using geogrid and lightweight aggregate (Bakeer et al., 1998b) | 16 |
| Figure 2. 3: Pull out capacity for corrugated strip (Recana et al.,2003) | 14 |
| Figure 2. 4: Geogrids used in pull out tests by Alagiyawanna et al., (2001) | 17 |
| Figure 2. 5: Result from pullout test for flexible and rigid reinforcement | 18 |
| Figure 2. 6: Results from inclined board test and large direct shear box tests involving 60 mm×60 mm geomembrane and geotextile interface | 19 19 |
| Figure 2. 7: Strip of different geometres (Recaca et al., 2003) | 21 |
| Figure 2. 8: Pullout capacity for horizontal strip (Recana et al., 2003) | |
| Figure 2. 11: Cases of bearing strength degradation (Palmeira, 2004) | 24 |
| Figure 2. 12: Pullout capacity against displacement of steel grid without triangular kinks (Tin et al., 2011) | 25 |
| Figure 2. 13: Pullout capacity of steel grid with 1 triangle kink (Tin et al., 2011) | 26 |

| | |
|--|----|
| Figure 2. 14: Pullout capacity of steel grid with 2 triangle kinks (Tin et al., 2011) | 28 |
| Figure 2. 15: Maximum pullout capacities in tests by Tin et al. (2011) | 27 |
| Figure 2. 16: Pull out apparatus as used by Abdi and Arjomand (2011) | 28 |
| Figure 2. 17: Results of pull out tests by Abdi and Arjomand (2011) | 29 |
| Figure 2. 18: Results of tests by Palmeira and Milligan (1989a): (a) influence by rigid or flexible top boundary; (b) influence by wall roughness | 30 |
| Figure 2. 19: Pullout interactions for (a) narrow and (b) wide reinforcement | 33 |
| Figure 2. 20: FEM of a pull out test by Khedkar and Mandal (2009) | 37 |
| Figure 2. 20: FEM of a pull out test by Khedkar and Mandal (2009) | 38 |
| Figure 2. 21: Failure zone in modelling by Khedkar and Mandal (2009) | 39 |
| Figure 2. 22: Comparison between experimental and FEM results (Duncan and Chang, 1970) | 40 |
| Figure 2. 23: Finite element mesh for a pull out test using SAGE CRISP software (Bergado et al., 2003) | 41 |
| Figure 2. 24: Results of modelling pull out tests using PLAXIS and SAGE CRISP involving galvanized strip | 44 |
| Figure 2.25: Diagrams of: (a) reinforced retaining wall and (b) equilibrium analytical forces associated with the retaining wall (Sawicki, A. (2000) | 44 |
| Figure 2. 26: Reinforcement strip model: (a) Reinforcing strip in ‘active’ and ‘resistant’ zones; (b) strip-soil interaction (Sawicki, A. (2000) | 45 |
| Figure 2. 27: Equilibrium of forces in reinforcement strip (Sawicki, A. (2000)) | 46 |

| | |
|--|----|
| Figure 2. 28: Failure zone of strip (Sawicki, A. (2000)) | 49 |
| Figure 2. 29: Active zone of reinforcement (Sawicki, A. (2000)) | 50 |
| Figure 3. 1: Strips fabricated for this research in lateral view | 59 |
| Figure 3. 2: Strips fabricated for this research in longitudinal view | 61 |
| Figure 3. 3: The machine used to cut longitudinal member and other parts of a strip | 64 |
| Figure 3. 4: Longitudinal member of a strip | 64 |
| Figure 3. 5: Strip with ribs on one side | 64 |
| Figure 3. 6: Strip with ribs on both sides | 65 |
| Figure 3. 7: Anchorage elements in stacks before being attached to longitudinal elements | 66 |
| Figure 3. 8: Stiffeners | 67 |
| Figure 3. 9: A strip with shearing elements strengthened by stiffeners | 68 |
| Figure 3. 10: Strip with shearing elements - 6 cm depth - and stiffeners on both sides | 68 |
| Figure 3. 11: Welding work being carried out | 70 |
| Figure 3. 12: A galvanizing work in being carried out | 72 |
| Figure 3. 13: Anchorage elements being soldered to the main plate by a technician. | 73 |
| Figure 3. 14: Specifications of a plate with no element | 75 |
| Figure 3. 15: Specifications of a plate with one element | 75 |

| | |
|--|----|
| Figure 3. 16: Specifications of a plate with two element | 76 |
| Figure 3. 17: Galvanized steel plate specifications with three elements | 76 |
| Figure 3. 18. Sieve analysis of soil | 77 |
| Figure 3. 19: Compaction test equipment | 80 |
| Figure 3. 20: Compaction curve for fill soil | 80 |
| Figure 3. 21: Tensile test equipment of the School of Civil Engineering, USM | 81 |
| Figure 3. 22: Monitoring system of the tensile test equipment | 82 |
| Figure 3. 23:Tensile test on plain strip | 83 |
| Figure 3. 24: Tensile test on strip with ribs on both side | 83 |
| Figure 3. 25: Tensile test on strip with one anchorage element of 6 cm deep | 84 |
| Figure 3. 26: Tensile test on strip with two anchorage elements of 6 cm deep | 84 |
| Figure 3. 27: The pressured cell of the Triaxial test apparatus | 85 |
| Figure 3. 28: Sample wrapped in rubber mounted onto the base of a triaxial cell | 86 |
| Figure 3. 29. Wrapped sample being mounted during preparation of a triaxial test | 87 |
| Figure 3. 30: Pull out apparatuses used in this study | 90 |
| Figure 3. 31. Compaction procedure in pull out box | 90 |

| | |
|--|-----|
| Figure 3. 32: Concrete block connector – strip connection in actual projects | 91 |
| Figure 3. 33: Pull rod – strip connection adopted for tests in this study | 92 |
| Figure 3. 34: Sleeve in pull out box | 92 |
| Figure 3. 35: Front strain gage | 93 |
| Figure 3. 36: Rear strain gage | 93 |
| Figure 3. 37: Manual for the front strain gage | 94 |
| Figure 3. 38: Manual for the rear strain gage | 95 |
| Figure 3. 39: Load cell for the pull out apparatuses | 95 |
| Figure 3. 40: Data logger for the pull out apparatuses | 96 |
| Figure 3. 41: Computer used with the pull out apparatuses | 97 |
| Figure 3. 42: Air bag positioned on top of soil in the pull out box | 97 |
| Figure 3. 43. Pressure gage for the airbag entrance | 99 |
| Figure 3. 44: Pressure gage next to air compressor | 99 |
| Figure 3. 45: A Direct shear test apparatus | 106 |
| Figure 3. 46: A plate with 3 anchorage elements lying on top of a base of direct shear box | 106 |
| Figure 4. 1: Strain versus stress curves for strips | 100 |
| Figure 4. 2: Displacement versus force curves for strips | 106 |

| | |
|---|-----|
| Figure 4. 3: Strain versus time curves for strips | 106 |
| Figure 4. 4: Front and back displacements versus pull out force for plain strip and $\sigma_n = 50$ kPa | 110 |
| Figure 4. 5: Front and back displacements versus time for plain strip and $\sigma_n = 50$ kPa | 111 |
| Figure 4. 6: Front and back displacements versus pull out force for plain strip and $\sigma_n = 75$ kPa | 111 |
| Figure 4. 7: Front and back displacements versus time for plain strip and $\sigma_n = 75$ kPa | 112 |
| Figure 4. 8: Front and back displacements versus pull out force for plain strip and $\sigma_n = 100$ kPa | 112 |
| Figure 4. 9: Front and back displacements versus time for plain strip and $\sigma_n =$ kPa | 113 |
| Figure 4. 10: Normal force versus pull out force for tests with plain strips | 113 |
| Figure 4. 11: Front and back displacements versus pull out force for strip with ribs on one side and $\sigma_n = 50$ kPa | 114 |
| Figure 4. 12: Front and back displacements versus time for strip with ribs on one side and $\sigma_n = 50$ kPa | 115 |
| Figure 4. 13: Front and back displacements versus pull out force for strip with ribs on one side and $\sigma_n = 75$ kPa | 115 |
| Figure 4. 14: Front and back displacements versus time for strip with ribs on one side and $\sigma_n = 75$ kPa | 116 |
| Figure 4. 15: Front and back displacements versus pull out force for strip with ribs on one side and $\sigma_n = 100$ kPa | 116 |
| Figure 4. 16: Front and back displacements versus time for strip with ribs on one side and $\sigma_n = 100$ kPa | 117 |
| Figure 4. 17: Normal force versus pullout force for strip with ribs on one side | 117 |
| Figure 4. 18: Force-Displacement curve for ribbed strip on two sides and $\sigma_n = 50$ kPa | 118 |

| | |
|--|-----|
| Figure 4. 19: Time-Displacement curve for ribbed strip on two sides and $\sigma_n = 50$ kPa | 119 |
| Figure 4. 20: Force-Displacement curve for ribbed strip on two sides, $\sigma_n = 75$ kPa. | 119 |
| Figure 4. 21: Time-Displacement curve for ribbed strip on two sides and $\sigma_n = 75$ kPa | 120 |
| Figure 4. 22: Force-Displacement curve for ribbed strip on two sides, $\sigma_n =$ kPa | 120 |
| Figure 4. 23: Time-Displacement curve for ribbed strip on two sides, and $\sigma_n = 100$ kPa | 121 |
| Figure 4. 24: Normal stresses and pullout force for ribbed strip on two side | 121 |
| Figure 4. 25: Force-Displacement curve on strip with $n=1$, $h= 2$ cm and $\sigma_n =$ kPa | 123 |
| Figure 4. 26: Time-Displacement curve on strip with $n=1$, $h= 2$ cm and $\sigma_n = 50$ kPa | 123 |
| Figure 4. 27: Force-Displacement curve on strip with $n=1$, $h= 2$ cm and $\sigma_n = 75$ kPa | 124 |
| Figure 4. 28: Time-Displacement curve on strip with $n=1$, $h= 2$ cm and $\sigma_n = 75$ kPa | 124 |
| Figure 4. 29: Force-Displacement curve on strip with $n=1$, $h= 2$ cm and $\sigma_n = 100$ kPa | 125 |
| Figure 4. 30: Time-Displacement curve on strip with $n=1$, $h= 2$ cm and $\sigma_n = 100$ kPa | 125 |
| Figure 4. 31: Normal stresses and pullout force for strip with $n=1$ and $h=2$ cm | 126 |
| Figure 4. 32: Increase in equivalent strip-soil angle of friction with changing strip specification (I) | 127 |
| Figure 4. 33: Front and back displacements versus pull out force for strip with one anchorage element of 4 cm depth and $\sigma_n = 50$ kPa | 128 |
| Figure 4. 34: Front and back displacements versus time for strip with one anchorage element of 4 cm depth and $\sigma_n = 50$ kPa | 129 |
| Figure 4. 35: Front and back displacements versus pull out force for strip with one | 129 |

| | |
|--|-----|
| Figure 4. 36: Front and back displacements versus time for strip with one anchorage element of 4 cm depth and $\sigma_n = 75$ kPa | 130 |
| Figure 4. 37: Front and back displacements versus pull out force for strip with one anchorage element of 4 cm depth and $\sigma_n = 100$ kPa | 130 |
| Figure 4. 38: Front and back displacements versus pull out force for strip with one anchorage element of 4 cm depth and $\sigma_n = 100$ kPa | 131 |
| Figure 4. 39: Normal force versus pullout force for strip with one anchorage element of 4 cm depth | 131 |
| Figure 4. 40. Force-Displacement curve on strip with $n=1$, $h= 6$ cm and $\sigma_n = 50$ kPa | 132 |
| Figure 4. 41. Time-Displacement curve on strip with $n=1$, $h= 6$ cm and $\sigma_n = 50$ kPa | 133 |
| Figure 4. 42. Force-Displacement curve on strip with $n=1$, $h= 6$ cm and $\sigma_n =$ kPa | 133 |
| Figure 4. 43. Time-Displacement curve on strip with $n=1$, $h= 6$ cm and normal stress of 75 kPa | 134 |
| Figure 4. 44. Force-Displacement curve on strip with $n=1$, $h= 6$ cm and $\sigma_n = 100$ kPa | 134 |
| Figure 4. 45. Time-Displacement curve on strip with $n=1$, $h= 6$ cm and $\sigma_n = 100$ kPa | 135 |
| Figure 4. 46. Normal stresses and pullout force for strip with $n=1$ and $h=6$ cm depth | 135 |
| Figure 4. 47. Force-Displacement curve on strip with $n=1$, $h= 8$ cm and $\sigma_n = 50$ kPa | 137 |
| Figure 4. 48. Time-Displacement curve on strip with $n=1$, $h= 8$ cm and $\sigma_n = 50$ kPa | 137 |
| Figure 4. 49. Force-Displacement curve on strip with $n=1$, $h= 8$ cm and normal stress of 75 kPa | 138 |
| Figure 4. 50. Time-Displacement curve on strip with $n=1$, $h= 8$ cm and $\sigma_n = 75$ kPa | 138 |
| Figure 4. 51. Force-Displacement curve on strip with $n=1$, $h= 8$ cm and $\sigma_n = 100$ kPa | 139 |

| | |
|---|-----|
| Figure 4. 52. Time-Displacement curve on strip with $n=1$, $h= 8\text{cm}$ and $\sigma_n = 100$ kPa | 139 |
| Figure 4. 53. Normal stresses and pullout force for strip with $n=1$ and $h=8$ cm | 140 |
| Figure 4. 54: Increase in equivalent strip-soil angle of friction with changing strip specification (II) | 141 |
| Figure 4. 55. Force-Displacement curve on strip with $n=2$, $h= 2\text{cm}$ and $\sigma_n =50$ kPa | 147 |
| Figure 4. 56. Time-Displacement curve on strip with $n=2$, $h= 2\text{cm}$ and $\sigma_n =50$ kPa | 147 |
| Figure 4. 57. Force-Displacement curve on strip with $n=2$, $h= 2\text{cm}$ and normal stress of 75 kPa | 148 |
| Figure 4. 58. Time-Displacement curve on strip with $n=2$, $h= 2\text{cm}$ and $\sigma_n =50$ kPa | 148 |
| Figure 4. 59. Force-Displacement curve on strip with $n=2$, $h= 2$ cm and normal stress of 100 kPa | 149 |
| Figure 4. 60. Time-Displacement curve on strip with $n=2$, $h= 2\text{cm}$ and $\sigma_n =100$ kPa | 149 |
| Figure 4. 61. Force-Displacement curve on strip with $n=2$, $h= 4$ cm and $\sigma_n =50$ kPa | 150 |
| Figure 4. 62. Time-Displacement curve on strip with $n=2$, $h= 4\text{cm}$ and $\sigma_n = 50$ kPa | 151 |
| Figure 4. 63. Force-Displacement curve on strip with $n=2$, $h= 4$ cm and $\sigma_n =75$ kPa | 151 |
| Figure 4. 64. Time-Displacement curve on strip with $n=2$, $h= 4\text{cm}$ and $\sigma_n =75$ kPa | 152 |
| Figure 4. 65. Force-Displacement curve on strip with $n=2$, $h= 4$ cm and $\sigma_n =100$ kPa | 152 |
| Figure 4. 66. Time-Displacement curve on strip with $n=2$, $h= 4\text{cm}$ and $\sigma_n =100$ kPa | 153 |
| Figure 4. 67. Normal stresses versus pullout force for strip with $n=2$ and $h=4$ cm | 154 |
| Figure 4. 68. Force-Displacement curve on strip with $n=2$, $h= 6$ cm and normal stress of 50 kPa | 155 |

| | |
|---|-----|
| Figure 4. 69. Time-Displacement curve on strip with $n=2$, $h= 6$ cm and $\sigma_n = 50$ kPa | 155 |
| Figure 4. 70. Force-Displacement curve on strip with $n=2$, $h= 6$ cm and $\sigma_n =75$ kPa | 156 |
| Figure 4. 71. Time-Displacement curve on strip with $n=2$, $h= 6$ cm and $\sigma_n =75$ kPa | 156 |
| Figure 4. 72. Displacement curve on strip with $n=2$, $h= 6$ cm and $\sigma_n = 100$ kPa | 157 |
| Figure 4. 73. Time-Displacement curve on strip with $n=2$, $h= 6$ cm and $\sigma_n =10$ kPa | 157 |
| Figure 4. 74. Normal stresses and pullout force for strip with $n=2$ and $h=6$ cm | 158 |
| Figure 4. 75. Displacement curve on strip with $n=2$, $h= 8$ cm and $\sigma_n =50$ kPa | 159 |
| Figure 4. 76. Time-Displacement curve on strip with $n=2$, $h= 8$ cm and $\sigma_n = 50$ kPa | 160 |
| Figure 4. 77. Displacement curve on strip with $n=2$, $h= 8$ cm and $\sigma_n =75$ kPa | 160 |
| Figure 4. 78. Time-Displacement curve on strip with $n=2$, $h= 8$ cm and $\sigma_n =75$ kPa | 161 |
| Figure 4. 79. Displacement curve on strip with $n=2$, $h= 8$ cm and $\sigma_n =100$ kPa | 161 |
| Figure 4. 80. Time-Displacement curve on strip with $n=2$, $h= 8$ cm and $\sigma_n =100$ kPa | 162 |
| Figure 4. 81. Normal stresses and pullout force for strip with $n=2$ and $h=8$ cm | 162 |
| Figure 4. 82: Increase in equivalent strip-soil angle of friction with changing strip specification (III) | 163 |
| Figure 4. 83. Displacement curve on strip with $n=3$, $h= 2$ cm and $\sigma_n =50$ kPa | 164 |
| Figure 4. 84. Time-Displacement curve on strip with $n=3$, $h= 2$ cm and normal stress of 50 kPa | 165 |

| | |
|---|-----|
| Figure 4. 85. Displacement curve on strip with $n=3$, $h= 2$ cm and $\sigma_n =75$ kPa | 165 |
| Figure 4. 86. Time-Displacement curve on strip with $n=3$, $h= 2$ cm and normal stress of 75 kPa | 166 |
| Figure 4. 87. Displacement curve on strip with $n=3$, $h= 2$ cm and $\sigma_n =100$ kPa | 166 |
| Figure 4. 88. Time-Displacement curve on strip with $n=3$, $h= 2$ cm and $\sigma_n = 100$ kPa | 167 |
| Figure 4. 89. Normal stresses versus pullout force for strip with $n=3$ and $h=2$ cm | 167 |
| Figure 4. 90. Displacement curve on strip with $n=3$, $h= 4$ cm and $\sigma_n =50$ kPa | 168 |
| Figure 4. 91. Time-Displacement curve on strip with $n=3$, $h= 4$ cm and normal stress of 50 kPa | 169 |
| Figure 4. 92. Displacement curve on strip with $n=3$, $h= 4$ cm and $\sigma_n =75$ kPa | 169 |
| Figure 4. 93. Time-Displacement curve on strip with $n=3$, $h= 4$ cm and $\sigma_n =75$ kPa | 170 |
| Figure 4. 94: Displacement curve on strip with $n=3$, $h= 4$ cm and normal stress of 100 kPa | 170 |
| Figure 4. 95. Time-Displacement curve on strip with $n=3$, $h= 4$ cm and $\sigma_n =100$ kPa | 171 |
| Figure 4. 96. Normal stresses and pullout force for strip with $n=3$ and $h=4$ cm | 171 |
| Figure 4. 97. Displacement curve on strip with $n=3$, $h= 6$ cm and $\sigma_n =50$ kPa | 172 |
| Figure 4. 98. Time-Displacement curve on strip with $n=3$, $h= 6$ cm and $\sigma_n =50$ kPa | 173 |
| Figure 4. 99. Displacement curve on strip with $n=3$, $h= 6$ cm and $\sigma_n =75$ kPa | 173 |
| Figure 4. 100. Time-Displacement curve on strip with $n=3$, $h= 6$ cm and $\sigma_n = 75$ kPa | 174 |
| Figure 4. 101. Displacement curve on strip with $n=3$, $h= 6$ cm and $\sigma_n = 100$ kPa | 174 |

| | |
|---|-----|
| Figure 4. 102. Time-Displacement curve on strip with $n=3$, $h= 6$ cm and normal stress of 100 kPa | 175 |
| Figure 4. 103. Normal stresses and pullout force for strip with $n=3$ and $h=6$ cm | 175 |
| Figure 4. 104. Displacement curve on strip with $n=3$, $h= 8$ cm and $\sigma_n = 50$ kPa | 176 |
| Figure 4. 105. Time-Displacement curve on strip with $n=3$, $h= 8$ cm and $\sigma_n = 5$ kPa | 177 |
| Figure 4. 106. Displacement curve on strip with $n=3$, $h= 8$ cm and $\sigma_n =75$ kPa | 177 |
| Figure 4. 107. Time-Displacement curve on strip with $n=3$, $h= 8$ cm and $\sigma_n =7$ kPa | 178 |
| Figure 4. 108. Displacement curve on strip with $n=3$, $h= 8$ cm and $\sigma_n =100$ kPa | 178 |
| Figure 4. 109. Time-Displacement curve on strip with $n=3$, $h= 8$ cm and $\sigma_n =1$ kPa | 179 |
| Figure 4. 110. Normal stresses and pullout force for strip with $n=3$ and $h=8$ cm | 179 |
| Figure 4. 111: Increase in equivalent strip-soil angle of friction with changing strip specification (IV) | 180 |
| Figure 4. 112. Displacement curve on strip with $n=4$, $h= 2$ cm and $\sigma_n = 50$ kPa | 181 |
| Figure 4. 113. Time-Displacement curve on strip with $n=4$, $h= 2$ cm and normal stress of 50 kPa | 181 |
| Figure 4. 114. Displacement curve on strip with $n=4$, $h= 2$ cm and $\sigma_n =75$ kPa | 182 |
| Figure 4. 115: Time-Displacement curve on strip with $n=4$, $h= 2$ cm and $\sigma_n =7$ kPa | 182 |
| Figure 4. 116. Displacement curve on strip with $n=4$, $h= 2$ cm and $\sigma_n =100$ kPa | 183 |
| Figure 4. 117. Displacement curve on strip with $n=4$, $h= 2$ cm and $\sigma_n =100$ kPa | 183 |

| | |
|--|-----|
| Figure 4. 118. Normal stresses versus pullout force for strip with $n=4$ and $h=2$ cm | 184 |
| Figure 4. 119. Displacement curve on strip with $n=4$, $h= 4$ cm and $\sigma_n =50$ kPa | 185 |
| Figure 4. 120. Displacement curve on strip with $n=4$, $h= 4$ cm and $\sigma_n =50$ kPa | 185 |
| Figure 4. 121. Displacement curve on strip with $n=4$, $h= 4$ cm and $\sigma_n = 75$ kPa | 186 |
| Figure 4. 122. Displacement curve on strip with $n=4$, $h= 4$ cm and $\sigma_n =75$ kPa | 186 |
| Figure 4. 123. Displacement curve on strip with $n=4$, $h= 4$ cm and normal stress of 100 kPa | 187 |
| Figure 4. 124. Displacement curve on strip with $n=4$, $h= 4$ cm and $\sigma_n = 100$ kPa | 187 |
| Figure 4. 125. Normal stresses versus pullout force for strip with $n=4$ and $h=4$ cm | 188 |
| Figure 4. 126. Displacement curve on strip with $n=4$, $h= 6$ cm and $\sigma_n =50$ kPa | 189 |
| Figure 4. 127. Displacement curve on strip with $n=4$, $h= 6$ cm and $\sigma_n =50$ kPa | 189 |
| Figure 4. 128. Displacement curve on strip with $n=4$, $h= 6$ cm and normal stress of 75 kPa | 190 |
| Figure 4. 129. Displacement curve on strip with $n=4$, $h= 6$ cm and $\sigma_n =75$ kPa | 190 |
| Figure 4. 130. Displacement curve on strip with $n=4$, $h= 6$ cm and normal stress of 100 kPa | 191 |
| Figure 4. 131. Displacement curve on strip with $n=4$, $h= 6$ cm and $\sigma_n =100$ kPa | 191 |
| Figure 4. 132. Normal stresses versus pullout force for strip with $n=4$ and $h=6$ cm | 192 |
| Figure 4. 133. Displacement curve on strip with $n=4$, $h= 8$ cm and $\sigma_n =50$ kPa | 193 |
| Figure 4. 134. Displacement curve on strip with $n=4$, $h= 8$ cm and $\sigma_n =75$ kPa | 193 |

| | |
|--|-----|
| Figure 4. 135. Displacement curve on strip with $n=4$, $h= 8$ cm and $\sigma_n = 100$ kPa | 194 |
| Figure 4. 136. Displacement curve on strip with $n=4$, $h= 8$ cm and $\sigma_n = 50$ kPa | 194 |
| Figure 4. 137. Displacement curve on strip with $n=4$, $h= 8$ cm and $\sigma_n =750$ kPa | 195 |
| Figure 4. 138. Displacement curve on strip with $n=4$, $h= 8$ cm and $\sigma_n =100$ kPa | 195 |
| Figure 4. 139. Normal stresses versus pullout force for strip with $n=4$ and $h=8$ cm.. | 196 |
| Figure 4. 140: Increase in equivalent strip-soil angle of friction with changing strip specification (V | 196 |
| Figure 4. 141: A comparison of results from various test series (a) Plain strip, strip with ribs on one side, strip with ribs on both sides, and strip with one anchorage elements (b) strip with 2 anchorage elements (c) strip with 3 anchorage elements and (d) strip with 4 anchorage elements | 198 |
| Figure 4. 142: Front and back displacements versus pull out force for strip with top and bottom anchorage elements of 2 cm depth ($n=2$, $h=2$ cm) and $\sigma_n =50$ kPa | 203 |
| Figure 4. 143: Front and back displacements versus time for strip with top and bottom anchorage elements of 2 cm depth ($n=2$, $h=2$ cm) and $\sigma_n = 50$ kPa | 203 |
| Figure 4. 144: Front and back displacements versus pull out force for strip with top and bottom anchorage elements of 4 cm depth ($n=2$, $h=4$ cm) and $\sigma_n =50$ kPa | 204 |
| Figure 4. 145: Front and back displacements versus time for strip with top and bottom anchorage elements of 4 cm depth ($n=2$, $h=4$ cm) and $\sigma_n =50$ kPa | 204 |
| Figure 4. 146: Front and back displacements versus pull out force for strip with top and bottom anchorage elements of 6 cm depth ($n=2$, $h=6$ cm) and $\sigma_n =50$ kPa | 205 |
| Figure 4. 147: Front and back displacements versus time for strip with top | 205 |

| | |
|--|-----|
| Figure 4. 148: Front and back displacements versus pull out force for strip with top and bottom anchorage elements of 6 cm depth (n=2, h=8 cm) and $\sigma_n = 50$ kPa | |
| Figure 4. 149: Front and back displacements versus time for strip with top and bottom anchorage elements of 6 cm depth (n=2, h=8 cm) and $\sigma_n = 50$ kPa | 206 |
| Figure 4. 150: Strip specification versus pull out capacity for strip with 2 anchorage elements (a) an anchorage element attached to top of strip and another at the bottom (b) both anchorage elements attached at the bottom | 207 |
| Figure 4. 151: Front and back displacements versus pull out force with elements of 2, 4, 6, and 8 cm depths attached to top and bottom of a strip (n=8, h=2,4,6, and 8 cm) and $\sigma_n = 100$ kPa | 209 |
| Figure 4. 152: Front and back displacements versus time with elements of 2, 4, 6, and 8 cm depths attached to top and bottom of a strip (n=8, h=2,4,6, and 8 cm) and $\sigma_n = 100$ kPa | 209 |
| Figure 4. 153: Strip specification versus pull out capacity for strip with various arrangements involving anchorage elements | 210 |
| Figure 4. 154: Front and back displacements versus pull out force with elements of 6 cm depths 2 attached to the top and 2 at the bottom of a strip (n=4, h=6 cm) and $\sigma_n = 100$ kPa | 211 |
| Figure 4. 155: Front and back displacements versus time with elements of 6 cm depths, 2 attached to the top and 2 at the bottom of a strip (n=4, h=6 cm) and $\sigma_n = 100$ kPa | 212 |
| Figure 4. 156: Strip specification versus pull out capacity for strip with various arrangements involving anchorage elements | 212 |
| Figure 4. 157. Performances of ribbed and plain strips | 214 |
| Figure 4. 158: Performance of Strips with 1 element | 215 |
| Figure 4. 159. Performance of Strips with 2 elements | 215 |

| | |
|--|-----|
| Figure 4. 160. Performance of Strips with 3 elements | 216 |
| Figure 4. 161. Performance of Strips with 4 elements | 216 |
| Figure 4. 162: Performance of Strips with h=2 cm | 217 |
| Figure 4. 163. Performance of Strips with h=4cm | 218 |
| Figure 4. 164: Performance of Strips with h=6 cm | 218 |
| Figure 4. 165: Performance of Strips with h=8 cm | 219 |
| Figure 4. 166: Photo showing plastic deformation involving strip with extra long anchorage element | 220 |
| Figure 4. 167: Effect of count divided by depth of elements on pull out capacity | 231 |
| Figure 4. 168: Relative change in pull out capacity with increasing height and count of elements | 222 |
| Figure 4. 169: Displacement versus shearing stress involving one shear element of various heights - $\sigma = 40$ kPa | 225 |
| Figure 4. 170: Displacement versus shearing stress involving 2 shear elements of various heights - $\sigma = 40$ kPa | 226 |
| Figure 4. 171: Displacement versus shearing stress involving three shear elements of various heights - $\sigma = 40$ kPa | 226 |
| Figure 4. 172: Effects of height of element on equivalent friction angel of various counts of elements | 228 |
| Figure 4. 173: Stress- strain curve from triaxial test | 228 |
| Figure 4. 174: Comparison of (F/P) Experimental and (F/P)Predicted | 236 |
| Figure 4. 175: Zones of horizontal displacement surrounding a plain strip under pull out loading | 238 |

| | |
|---|-----|
| Figure 4. 176: Shear stress zones surrounding a plain strip under pull out loading | 238 |
| Figure 4. 177: Deformed mesh surrounding a plain strip under maximum pull out loading corresponding to maximum displacement of 10.37 mm | 239 |
| Figure 4. 178: Stress points showing principal stresses surrounding a plain strip under pull out loading | 239 |
| Figure 4. 179: Zones of displacement surrounding a strip with an anchorage element of 2 cm deep under pull out loading | 241 |
| Figure 4. 180: Stress zones surrounding a strip with an anchorage element of 2 cm deep under pull out loading | 242 |
| Figure 4. 181: Deformed mesh surrounding a strip with 2 cm deep anchorage element under pull out loading | 242 |
| Figure 4. 182: Stress points showing principal stresses surrounding a strip with 2 cm anchorage element under pull out loading | 243 |
| Figure 4. 183: Zones of displacement surrounding a strip with an anchorage element of 4 cm deep under pull out loading | 243 |
| Figure 4. 184: Stress zones surrounding a strip with an anchorage element of 4 cm deep under pull out loading | 244 |
| Figure 4. 185: Deformed mesh of strip with one anchorage element and 4 cm height under maximum pullout force | 244 |
| Figure 4. 186: Stress points showing principal stresses surrounding a strip with 4 cm anchorage element under pull out loading | 245 |
| Figure 4. 187: Zones of displacement surrounding a strip with an anchorage element of 6 cm deep under pull out loading | 245 |
| Figure 4. 188: Stress zones surrounding a strip with an anchorage element of 6 cm deep under pull out loading | 246 |
| Figure 4. 189: Deformed mesh of strip with one anchorage element and 6 cm height under maximum pullout force | 246 |
| Figure 4. 190: Stress points showing principal stresses surrounding a strip with 6 cm anchorage element under pull out loading | 247 |
| Figure 4. 191: Zones of displacement surrounding a strip with an anchorage element of 8 cm deep under pull out loading | 247 |
| Figure 4. 192: Stress zones surrounding a strip with an anchorage element of 8 cm | 248 |

| | |
|--|-----|
| Figure 4. 193: Deformed mesh surrounding a strip with 8 cm deep anchorage element under pull out loading | 248 |
| Figure 4. 194: Stress points showing principal stresses surrounding a strip with 8 cm anchorage element under pull out loading | 249 |
| Figure 4. 195: Zones of displacement surrounding a strip with 2 anchorage elements of 2 cm deep under pull out loading | 252 |
| Figure 4. 196: Stress zones surrounding a strip with 2 anchorage elements of 2 cm deep under pull out loading | 252 |
| Figure 4. 197. Deformed mesh surrounding a strip with 2 anchorage elements of 2 cm depth under pull out loading | 253 |
| Figure 4. 198: Stress points showing principal stresses surrounding a strip with 2 anchorage elements of 2 cm depth under pull out loading | 253 |
| Figure 4. 199. Zones of displacement surrounding a strip with 2 anchorage elements of 4 cm deep under pull out loading | 254 |
| Figure 4. 200. Stress zones surrounding a strip with 2 anchorage elements of 4 cm deep under pull out loading | 254 |
| Figure 4. 201. Deformed mesh surrounding a strip with 2 anchorage elements of 4 cm depth under pull out loading | 255 |
| Figure 4. 202: Stress points showing principal stresses surrounding a strip with 2 anchorage elements of 4 cm depth under pull out loading | 255 |
| Figure 4. 203. Zones of displacement surrounding a strip with 2 anchorage elements of 6 cm deep under pull out loading | 256 |
| Figure 4. 204. Stress zones surrounding a strip with 2 anchorage elements of 6 cm deep under pull out loading | 256 |
| Figure 4. 205. Deformed mesh surrounding a strip with 2 anchorage elements of 6 cm depth under pull out loading | 257 |
| Figure 4. 207: Zones of displacement surrounding a strip with 2 anchorage elements of 8 cm deep under pull out loading | 258 |
| Figure 4. 208: Stress zones surrounding a strip with 2 anchorage elements of 8 cm deep under pull out loading | 258 |
| Figure 4. 209: Deformed mesh surrounding a strip with 2 anchorage elements of 8 cm depth under pull out loading | 259 |

| | |
|--|-----|
| Figure 4. 210: Stress points showing principal stresses surrounding a strip with 2 anchorage elements of 8 cm depth under pull out loading | 259 |
| Figure 4. 211: Failure zone of strip with three anchorage element and 2 cm height under pull out force in horizontal direction | 261 |
| Figure 4. 212: Failure zone in x-y direction of pull out force in strip with three anchorage element and 2 cm height | 261 |
| Figure 4. 213: Deformed mesh of strip with tow anchorage element and 2 cm height under maximum pullout force | 262 |
| Figure 4. 214: Stress point in pullout box under over pressure and pull out force | 262 |
| Figure 4. 214: Stress point in pullout box under over pressure and pull out force | 263 |
| Figure 4. 215: Failure zone of strip with three anchorage element and 4 cm height under pull out force in horizontal direction | 263 |
| Figure 4. 215: Failure zone of strip with three anchorage element and 4 cm height under pull out force in horizontal direction | 264 |
| Figure 4. 216: Failure zone in x-y direction of pull out force in strip with three anchorage element and 4 cm height | 264 |
| Figure 4. 217: Deformed mesh of strip with tow anchorage element and 4 cm height under maximum pullout force | 265 |
| Figure 4. 218: Stress point in pullout box under over pressure and pull out force | 265 |
| Figure 4. 219: Failure zone of strip with three anchorage element and 6 cm height under pull out force in horizontal direction | 266 |
| Figure 4. 220: Failure zone in x-y direction of pull out force in strip with three anchorage element and 4 cm height | 267 |
| Figure 4. 221: Deformed mesh of strip with tow anchorage element and 6 cm height under maximum pullout force | 267 |
| Figure 4. 222: Stress point in pullout box under over pressure and pull out force | 268 |
| Figure 4. 223: Failure zone of strip with three anchorage element and 8 cm height under pull out force in horizontal direction | 268 |
| Figure 4. 224: Failure zone in x-y direction of pull out force in strip with three | 271 |

| | |
|---|-----|
| anchorage element and 8 cm height | |
| Figure 4. 225: Deformed mesh of strip with tow anchorage element and 6 cm height under maximum pullout force | 271 |
| Figure 4. 226: Stress point in pullout box under over pressure and pull out force | 272 |
| Figure 4. 227. Failure zone of strip with four anchorage element and 2 cm height under pull out force in horizontal direction | 272 |
| Figure 4. 228. Failure zone in x-y direction of pull out force in strip with four anchorage element and 2 cm height | 273 |
| Figure 4. 229. Deformed mesh of strip with four anchorage element and 4 cm height under maximum pullout force | 272 |
| Figure 4. 230. Stress point in pullout box under over pressure and pull out force | 272 |
| Figure 4. 231. Failure zone of strip with four anchorage element and 6 cm height under pull out force in horizontal direction | 273 |
| Figure 4. 231. Failure zone of strip with four anchorage element and 6 cm height under pull out force in horizontal direction | 273 |
| Figure 4. 232. Failure zone in x-y direction of pull out force in strip with four anchorage element and 4 cm height | 273 |
| Figure 4. 233. Deformed mesh of strip with four anchorage element and 4 cm height under maximum pullout force | 274 |
| Figure 4. 234. Stress point in pullout box under over pressure and pull out force | 274 |
| Figure 4. 235. Failure zone of strip with four anchorage element and 6 cm height under pull out force in horizontal direction | 275 |
| Figure 4. 236. Failure zone in x-y direction of pull out force in strip with four anchorage element and 6 cm height | 275 |
| Figure 4. 237. Deformed mesh of strip with four anchorage element and 6 cm height under maximum pullout force | 276 |
| Figure 4. 238. Stress point in pullout box under over pressure and pull out force | 276 |
| Figure 4. 239. Failure zone of strip with four anchorage element and 8 cm height under pull out force in horizontal direction | 277 |

| | |
|---|-----|
| Figure 4. 240. Failure zone in x-y direction of pull out force in strip with four anchorage element and 8 cm height | 277 |
| Figure 4. 241. Deformed mesh of strip with four anchorage element and 8 cm height under maximum pullout force | 278 |
| Figure 4. 242. Stress point in pullout box under over pressure and pull out force | 278 |
| Figure 4.243: Maximum horizontal displacement versus maximum shear stress | 282 |
| Figure 4.244: Maximum horizontal displacement versus maximum shear stress | 283 |
| Figure 4.245: Redistribution of stressed regions by changing count of anchorage elements (a) no anchorage element (b) one anchorage element (c) 2 anchorage element (d) 3 anchorage elements (e) 4 anchorage elements | 284 |
| Figure 4.246: Redistribution of stressed regions by changing count of anchorage elements (a) no anchorage element (b) one anchorage element (c) 2 anchorage element (d) 3 anchorage elements (e) 4 anchorage elements | 286 |
| Figure 4.247: Redistribution of stressed regions by changing count of anchorage elements (a) no anchorage element (b) one anchorage element (c) 2 anchorage element (d) 3 anchorage elements (e) 4 anchorage elements | 287 |

LIST OF SYMBOL

PR_s = Pull out capacity of skin friction in reinforcement

PR_b = Pull out capacity of transverse ribs in reinforcement

α_s = Fraction of reinforcement surface which is solid

LR = Length of specimen

σ_n = Normal stress

δ = Interface friction angle

S = Distance between transverse members

$\alpha\beta$ = Fraction of total frontal area of reinforcement available for bearing

h = Depth of anchorage element

n = Count of anchorage element

σ_b = Passive bearing of transverse member in soil

fb = Pull out interaction of soil-reinforcement

ϕ = Friction angle of soil

$Nt = \left(\frac{LR}{S}\right)$ = Length divided to distance of transverse member

Ntb = node number in transverse elements

Ab = area of each rib element (single node and bar between two nodes)

Nq = Bearing resistance factor for transverse members

F_1 = "Ultimate frictional of all longitudinal ribs"

F_2 = "Ultimate frictional resistance of all transverse ribs"

F_3 = "ultimate bearing resistance of all transverse ribs"

A_l = surface of longitudinal members

A_t = surface of transverse ribs

A_b = bearing surface of ribs

f = Pull out resistance factor

α = correction coefficient of nonlinear shear stress distribution on reinforcement

($\alpha = 1$ for metal strip)

σ_n = Vertical normal stress

Le = Effective length of strip

B = Weight of strip

C = Effective unit of perimeter on strip

f = adherence coefficient of soil – geogrid

α = scale correction factor

e = thickness of transverse rib

s = transverse ribs spacing

αs = ratio between the plane area of geogrids (transverse and longitudinal)

αp = " Ratio between transverse element where in passive resistance is fully moved and corresponding total area"

$\frac{\phi_s}{GGR}$ = soil-geogrids friction angle

M = Mass

L = length

T = time

τ_{max} = maximum shearing force

σ_n = normal stress

D_{10} = Particle diameter soil size that 10 % passing

D_{30} = Particle diameter soil size that 30 % passing

D_{50} = Particle diameter soil size that 50 % passing

D_{60} = Particle diameter soil size that 60 % passing

G_s = Specific gravity

e_{min} = Minimum void ratio

e_{max} = Maximum void ratio

USCS Classification = unified soil classification system

γ_d = Maximum Dry Unit Weight

w = Optimum moisture content

C_u = Coefficient of Uniformity

C_c = Coefficient of Curvature

ϕ = Angle of Friction

D_r = Relative density of soil

Ψ = Dilatancy angle of soil

KAJIAN KESAN UNSUR SAUH KEATAS KEKUATAN TARIK KELUAR JALUR TETULANG DALAM PASIR

ABSTRAK

Sudut ricih permukaan di antara dua jenis bahan suatu parameter yang sangat penting dalam rekabentuk tanah terstabil mekanikal (MSE) kerana ianya berkait terus dengan keupayaan rintangan tarik keluar jalur pengukuh. Dalam penyelidikan ini, anggota sauh telah ditambah keatas jalur pengukuh bagi meningkatkan sudut ricih permukaan dan keupayaan rintangan tarik keluar. Pasir digunakan sebagai bahan isi. Dalam ujian yang dijalankan, satu jalur licin, dua jalur dengan rasuk mudah, dan lapan belas jalur beranggota melintang dengan berbagai kedalaman dan bilangan telah dikenakan beban tarik keluar dengan tegasan pugak berjulat 50 kPa hingga 100 kPa. Teorem π -Buchingham dan analisis regresi menggunakan perisian statistik – SPSS v.14 – telah juga digunakan bagi menentukan persamaan am yang mengaitkan antara keupayaan rintangan tarik keluar dengan parameter jalur, dan membandingkan diantara kekuatan anggaran dengan keputusan sebenar ujian. Hasil kajian mendapati bahawa kaedah baru melibatkan anggota sauh boleh memberi penjimatan penggunaan jalur atau rekabentuk MSE tertentu yang sesuai digunakan bagi ruangan sempit, lantaran peningkatan rintangan tarik keluar bagi setiap jalur boleh mengurangkan panjang keseluruhan atau jumlah bahan yang diperlukan dalam setiap projek. Dalam kajian ini juga, radas ujian rich terus telah digunakan bagi menentukan rintangan ricih permukaan diantara sampel pamsir terged baik dengan

plat keluli tergalvani. Akhir sekali, pemodelan unsur terhingga telah dijalankan bagi melengkapkan analisis. Keputusan ujian tarik keluar yang digabungkan dengan keputusan pemodelan didapati sangat berguna bagi jurutera menentukan rekabentuk terbaik struktur tanah terkukuh.

INFLUENCE OF TRANSVERSE ELEMENTS ON THE PULLOUT CAPACITY OF METAL STRIP REINFORCEMENT IN SANDY SOIL

ABSTRACT

Interface friction angle between different materials is a very important parameter in the designs of mechanically stabilized earth (MSE) as it corresponds directly to pull out capacity of a reinforcement strip. In this research, anchorage elements have been added to normal reinforcement strip in order to increase interface friction angle and thus the pull out capacity. Sand was used as fill material. In the tests, one plain strip with smooth surface, two strips with simple ribs, and eighteen strips with transverse members of various depths and counts were subjected to pull out forces with normal stresses ranging from 50 kPa to 100 kPa applied. Also, π -Buchingham theorem and regression analysis using statistical software - SPSS v.14 - were used to obtain general equations relating pull out capacity to strip parameters and compare predicted strength values to actual outcomes of the tests. The results of the study indicate that the new method involving transverse members could generally offer saving of strip material or provide particular design criteria for MSE of limited construction space, since the increased capacity of each reinforcement strip would reduce the total length or amount of strips required in a project. Also in this research, direct shear apparatus used for soil testing was employed to measure the interface

shear resistance between well graded sand samples and galvanized steel plates. Finally, finite element computer modelling with Plaxis V 8.2 software was carried out to complete the analyses. The results from pull out tests combined with results from the modelling were found to be very useful for engineers to design better reinforced earth structures.

CHAPTER 1

INTRODUCTION

1.1 Introduction

Since the first installation of MSE by Vidal in 1961, the structure which is also known as either reinforced retaining wall, reinforced embankment, or reinforced soil, depending on the application, has been widely used in geotechnical projects where it provides a low-strain, strong, and durable solution for stabilization of fill or original material of the site (Bergado et al., 1987). Reinforced earth (Gurung, 2001) is made by reinforcing the soil with tension member like bar, steel plate, galvanized stripes, and geo-membranes. Reinforcement materials are categorized as either extensible such as the geotextiles and the geogrids or inextensible such as the metal strips and the metal grids; tests and analyses have been carried out involving both (Ochiai et al.,1996; Khedkar and Mandal, 2009 and Balunaini and Prezzi, 2010). Interface friction angles between reinforcement materials and soils have been determined, the effects of various geometrical arrangements have been evaluated, and efforts have been made at having the reinforcement strips shortened while maintaining the required pull capacity such as by having the strips corrugated instead of plain (Potyondy, 1961; Zhang et al., 2008; and Racana et al., 2003).

Design of the MSE wall component of an MSE wall system should consider:

- Internal stability of the reinforced soil mass with regard to rupture and pullout of reinforcing elements such as pullout rupture of reinforcement and interface friction angle.
- External stability along the MSE wall/shoring wall interface such as friction between soil and MSE wall.
- Bearing capacity and settlement of the MSE wall foundation materials.
- Global stability of the composite SMSE wall system.

Generally speaking, the generic term ‘reinforced earth’ or ‘reinforced soil’ is used to describe all types of earth structures strengthened by reinforcements. However, in the industry, a large majority of reinforced earths has come under the more formal name category known as the mechanically stabilized earth or in short, MSE. Henry Vidal has been said as the inventor of the MSE (Haeri et al., 2000). Since the first installation of MSE by Vidal in 1961, the structure which also refers to reinforced retaining wall, reinforced embankment, and reinforced soil, depending on the application, has been widely used in geotechnical projects where it provides a low-strain, strong, and durable solution for stabilization of fill or original material of the site. In a MSE structure, reinforcement strips which are either metallic or synthetic, and plain or ribbed, are placed horizontally in the midst of layers of granular soil that is normally used as backfill or embankment material. Recent experiments and experiences involving MSE have been reported by many researchers (Varuso et al., 2005; Bathurst et al., 2005; Skinner and Rowe 2005; Hufenus et al., 2006; Nouri et al., 2006; Chen et al., 2007; Bergado and

Teerawattanasuk, 2008; Li and Rowe, 2008; Sieira et al., 2009; Palmeira, 2009; Abdelouhab et al., 2010).

Figure 1.1 is profile of a MSE as commonly installed today for road embankments where they apply. Inside the failure wedge, the reinforcement improves tension weaknesses in the soils, while across the potential slip surface, in the adjacent anchoring ground, the reinforcement holds the wedge against sliding or translational failure by having strips extended into the ground. For getting design parameters, pull-out tests are normally carried out. The pullout mechanisms of various reinforcement strips have been investigated not only by full-scale and laboratory model tests, but also by numerical methods (Palmeira and Milligan, 1989; Alagiyawanna et al., 2001; Gurung, 2001; Moraci and Cardile, 2009; Abdi and Arjomand, 2011; Goodhue et al., 2001; Sugimoto, 2003; Desai and Hoseiny, 2005; Moraci and Gioffre', 2006; Subaida et al., 2008; Su et al., 2008; Yin et al., 2008; Abdi et al., 2009; Zhou et al., 2011; Moraci and Cardile, 2012).

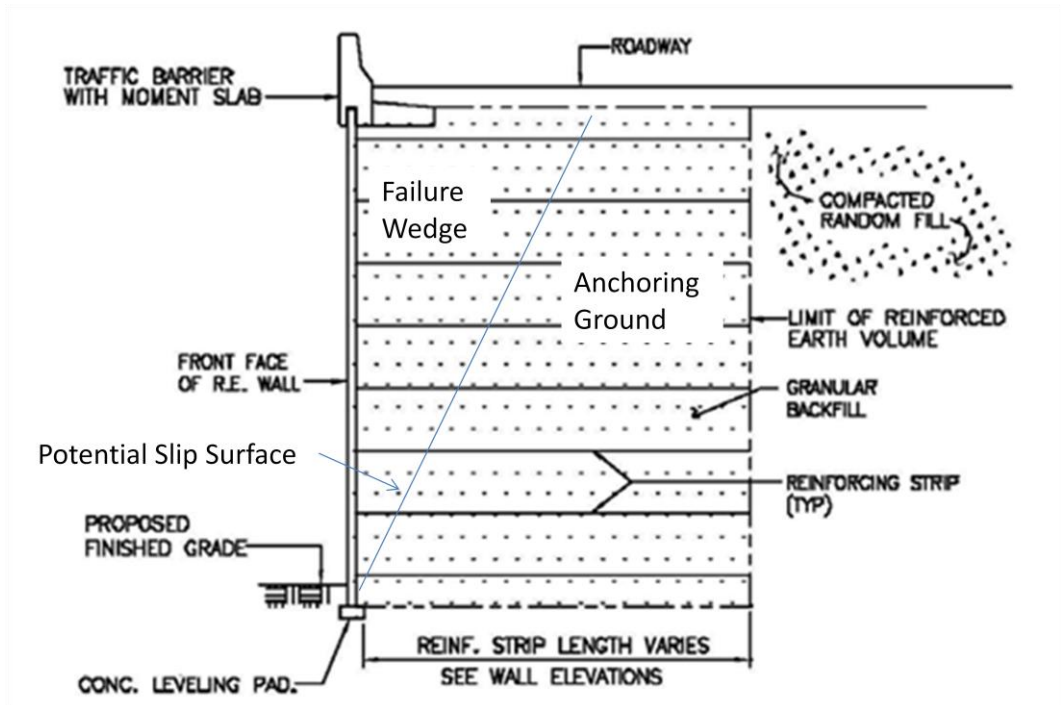


Figure 1.1: A profile of a commonly installed mechanically reinforced earth.(Sawicki, 2000)

1.2 Applications in Malaysia and abroad

The application of reinforced soil went back to ancient time, but since 1966 the method has been reinvented for design of reinforced retaining wall (Shukla et al., 2009). In the international arena of modern times, the use of reinforced retaining wall intensified in the 1980s and 1990s (Walls, 2009). In Malaysia, where soil reinforcement methods have been widely used in geotechnical projects, the use of reinforced earth for various geotechnical structures has become very popular in recent years. They can provide a low-strain, strong, and durable solutions for the stabilization of soils. From the front, outside of the reinforcement volume, view like shown in Figure 1.2 has become common sights in the country.

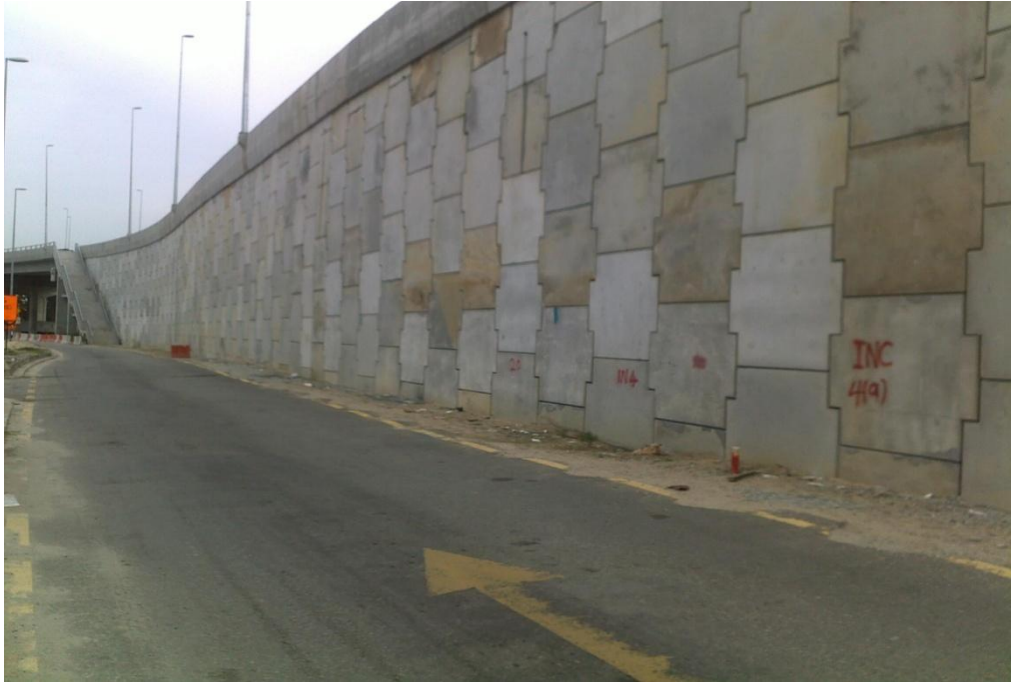


Figure 1.2: A view of MSE from the front showing decorative facing.

Inside the reinforcement volume, the interface friction angle between different materials is a very important factor in the design. The interface frictions between sand and galvanized steel is less than those between sand and sand because of the smooth surface of galvanized steel. Potyondy and Eng (1961) used smooth and rough materials, such as steel, wood, and concrete, to determine the interface friction between soil and these materials, restricting the moisture content and different normal loads between material and soil to find the interface friction of surfaces. The roughness of the steel, grain size of SW, and type of SW has been found to have an important effect on friction between two materials (Vesugi and kishida, 1981). Kishida et al. (1987) conducted some tests on the sand–steel interface using a simple apparatus and compared the results with those using others conventional apparatuses, such as direct shear test, annular shear test, and ring torsion experimental on the sand–plates interface; they compared the final results with those of other

experiments. The hardness of a material is the amount of surface resistance to the permanent indentation and may be considered a measure of the material strength. Hardness depends on both the geometry of the indenter and the material properties, including yield stress and bulk modulus. Moreover, it is not a true material property but rather a measurement. All materials with a low hardness amount have a high interface friction angle (Frost et al., 2002). Zhang et al. conducted a triaxial test to evaluate the interaction of horizontal-vertical orthogonal elements with sand and compared it with the ordinary horizontal type (Zhang et.al, 2008).

1.3 Recent trends in the use of geosynthetics

The recent development in the industry has found increased use of geosynthetics – geomembrane, geotextile, geogrids – in replacing more traditional reinforcements made of metal strips, timbers, and geofabrics.

When geomembrane is used, soil interface parameter (δ) and shear strength of a smooth geomembrane–soil interface are discussed as in many studies by different researchers. Interface testing procedures and their effects on measured interface strength parameters have been investigated by Takasumi et al. (1991) and Fishman and Pal (1994). They gave a comprehensive review of the geomembrane–soil interface characteristics (Fleming et al., 2006).

When geotextile and geogrids are used, friction between soil and the geosynthetics materials facilitates the simple interface shear resistance of the soil against them - soil particles are not really engaged in the small space of the thin

geosynthetics sheet. However, the direct shear resistance is more complex for the thicker and more gripping geogrid. The wider ribs and soil contact enable greater interface shear resistance. At the same time, the friction resistance of soil particles on the top and bottom of the geogrid occurs within geogrid apertures. Therefore, the shear resistance of the soil–geogrid interface contains at least the shear resistance between soil and the surface of geogrids ribs and the internal shear resistance of the soil in the spaces of the geogrid. Interface between the granular fills and geogrid strip reinforcements in order to measure bearing resistance between the geogrid and soils have been studied by other researchers (Lin et al., 2005).

Yildize wasti et al., (2001) studied the subject by conducting the shearing test on PVC geomembranes, smooth and rough HDPE, nonwoven needle-punched geotextiles with 5–50 KPa range of normal stress, inclined board tests, and different sizes of interface surfaces. The length of reinforcement plate could be decreased by increasing the friction between the soil and reinforcement material, reducing the cost of soil reinforcing projects.

In future, with increased use in geogrid type of geosynthetics, but with thicker diameter threads, the knowledge on how resistance could be increased by having protrusions and shear elements is needed. In the study to be described next, the interface friction between sand and galvanized steel plate is increased by adding extra elements to the galvanized plate. The effect of different sizes and geometries of

shearing elements is evaluated using pull out tests, direct-shear tests, and Finite element modelling using Plaxis software.

1.4 Problem Statement

MSE has been widely used and the future is expected to see more usage including for narrow and complicated spaces where limitation of strips length is necessarily. Limitation on the use of strips is also caused by economy – the lesser the strips, the cheaper would the constructions be in terms of cost. However, with smaller number of strips used in an MSE, the force associated with a single strip becomes more, which in turn is affecting the mechanisms of tying the strip against the segmental concrete crust. In order to increase reinforcement capacity per strip, changing the geometry of the strip could be the solution.

In fact, the results of this study indicate that the new method involving transverse members could generally offer saving of strip material or provide particular design criteria for MSE of limited construction space, since the increased capacity of each reinforcement strip would reduce the total length or amount of strips required in a project. The test program described in this research was another attempt at having shorter or lesser number of strips involving inextensible material. The transverse members, also called anchorage elements, with element stiffeners, are part of a direct and simple means of improving anchorage through having rigid protrusions positioned 90 degrees to the direction of potential movement. The

expected outcomes were saving in strip material and new design criteria of MSE for narrow or limited construction spaces.

1.5 Objectives of the research

1. To develop new strip for narrow place, with more pullout capacity and therefore economic benefits for projects.
2. To determine optimum depth of anchorage with given anchorage spaces or alternatively speaking, optimum anchorage distance for given anchorage depth.
3. To formulate pullout capacity for various given parameters based on pullout experimental results.
4. To study failure surfaces in soil reinforced with strips of various design and test conditions using finite element method (Plaxis software).

1.6 Scope of Research

This research proposed to investigate the results to pull out capacity of strips with new geometries for mechanically stabilized earth, as would be applicable in walls in narrow or complicated spaces. Furthermore this research will utilise strips with different geometrise in pullout tests and carry out interface direct shear and direct pull out tests with different normal stresses. Statistical analysis and finite element modelling are needed to estimate final pull out strengths and investigate failure surface and behaviour of anchorage elements in the pullout tests.

1.7 Structure of Thesis

This thesis is presented in five (5) chapters. First chapter introduces the research, objectives, problem statement, and scope. A review of previous study on pullout capacity and interface interactions, interface direct shear tests, past theories and experiments, and finite element methods are presented in Chapter 2. Chapter 3 presents research methodology implemented in this research. In chapter 4, results and discussion of tensile tests, pullout tests, interface direct shear tests, triaxial tests, and compaction tests are discussed. Finally the conclusion and recommendation for future work are presented in chapter five.

CHAPTER 2

LITERATURE REVIEW

2.1 Introduction

The research and industry of reinforced earth are generally more concerned with reinforcement material than with the earth fill material. The reinforcement materials, in turn, are comprised of steel and geosynthetics. The related tests carried out on these reinforcements are mainly the pull out tests and the direct shear tests. Computer modelling is carried out to corroborate the results. Pull out test and direct shear test are tow important experimental to investigate on soil and other material interface. For active zone of colomb failure surface and passive zone of MSE based on Mohr- colomb criteria direct shear test and pullout test are employed.

2.2 Pull out and direct shear tests involving reinforcement material

In study by Bakeer et al. (1998b), pull out test and interface shear test on geogrids were carried out against light aggregate with different confining pressures. In this study, the friction angles from pull out test was 52 degrees while from

interface friction test was 48 degrees, as given in Figure 2.1 and 2.2. Also, they found that some crushing actually had happened to the reinforced material with higher normal loads (Bakeer et al., 1998b).

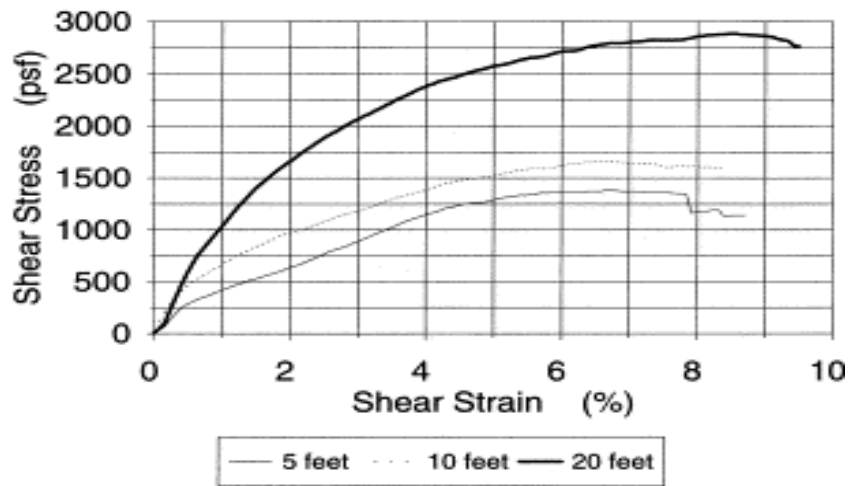


Figure 2.1: Results from pull out tests using geogrid and lightweight aggregate (Bakeer et al., 1998b)

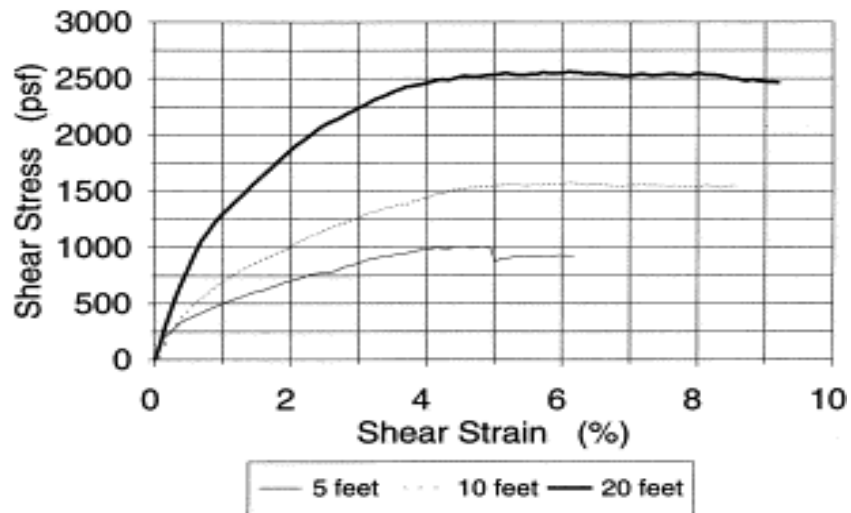


Figure 2.2: Results from interface shear tests using geogrid and lightweight aggregate (Bakeer et al., 1998b)

Boundary condition on pull out results was studied by Palmeira and Milligan (1989b). In this study, the results showed that certain friction on the inside of front wall of test box made it hard to predict the internal friction angle between soil and reinforcement material. They found that a larger scale pull out box and lubricating would be better in getting more accurate friction coefficient between materials.

In a study by Bergado et al. (1987), the interaction between soil and geogrids by using both direct shear and pull-out tests was investigated and the results were applied in a case study. Two types of Thailand soil - clayey sand and weathered clay – were used as backfill together with two types of reinforcement - polymer geogrid and bamboo grids. They found that the strength between soil and reinforcement has come from two factors: (a) the adhesion between soil and reinforcement on the solid surface area of the geogrid; and (b) the bearing withstand of soil in the fronts of the transverse members of geogrid that acted as a strip footing embedded in the soil. The design procedure for pull-out resistance coincided really well with the laboratory pull-out test results. Also their results showed that bamboo grids had higher pull-out resistance per unit area than the polymer geogrids. Furthermore, cohesive fills were found to be totally effective when used with geogrid reinforcement. Towards the end of their study, the results were applied in a design procedure to a case study involving an irrigation canal bank being repaired by the Public Works in Thailand. With Tensar SS2 geogrids as reinforcement and cohesive soils as backfill, a much improved embankment with very satisfactory slope stability was achieved.

Wilson Fahmy et al. (1994) carried out an investigations involving extensible reinforcement and dense sand in a series of pull out tests. They found that failures could take place by either sheet pull out or tension failure in the fill material. They have suggested that a great portion of pull out capacity was provided by the transverse elements thus the role of junctions in the reinforcement grids was very important. Also, the flexural capacity of traverse elements and the longitudinal extensibility of reinforcement should be considered as the main factor affecting the design involving this type of reinforcement.

A series of pull out tests have been carried out on extensible reinforcement and cohesion less soil by Oostveen et al. (1994). The results emphasized that front wall proximity was an important factor for the type of stress distribution on reinforcement - as suggested earlier by Palemira amd Miligan (1989).

Geogrids with various specifications and lengths were used in pull out tests by Frsman and Slunga (1994) in crushed rock, light clay aggregate, and sand material. Their results showed that, in a pull out test, when length of strips was increased, the average shear resistance was decreased because of progressive failure along the length of geogrid. With longer strip length, the lesser rigid would be the strip parts. Their results emphasized the roles of various factors such as strength of junction, rigidity of transverse bearing members, reinforcement strength, and modulus of deformation, on the pull out-displacement relationship.

According to Gurung and Iwao (1999), pull-out tests are widely employed to measure the soil-reinforcement interface interaction mechanism. They founded a simplified analysis for evaluation of the interaction mechanism in a general pull-out test which is proposed for geo-reinforcement. They also have done numerical studies for pull-out tests of different strains (large and small) for each type of inextensible to extensible reinforcements. They also have made comparison between the steel geostrap and polymer strip to verify the theories on both extensible and inextensible reinforcements. These researches have produced experimental and theoretical pull-out test results for various materials such as geotextiles, polymers, nylon geosynthetics and steel strip reinforcements. The predictions of pull out capacities were based from the models and their satisfactory comparisons with experimental results. The incorporated bi-linear relation allowed prediction of pre and post yield deformations, tensile force, and shear stress variations along the required length of the reinforcement.

In general, reinforcements are categorized in two major types, inextensible and extensible. Galvanized metal strips (straps), rock bolt, steel grids are called inextensible while geosynthetics, fibres, and polymers are called extensible reinforcement according their large strains resulted in pull out tests, as shown in Figure 2.3 (Gurung, 2001).

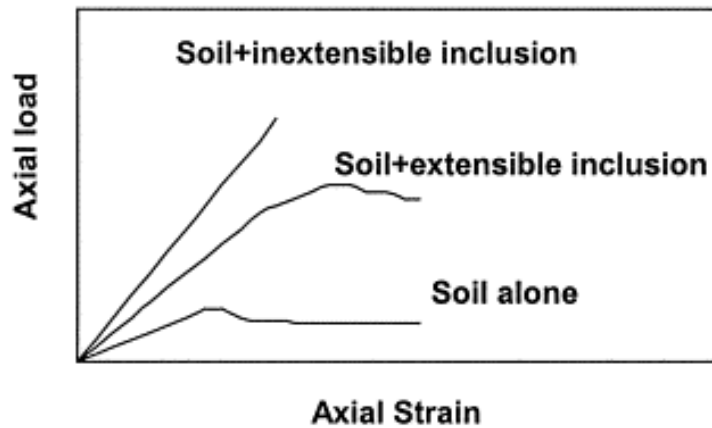


Figure 2.3: Description for inextensible and extensible reinforcements (Gurung, 2001))

Alagiyawanna et al. (2001) carried out pull out tests using extensible geogrid with high strain of geometries as shown in Figure 2.4. Their results indicate that in case on extensible reinforcement, longitudinal members were more significant member in providing the required pull out capacity in comparison to the lateral bearing member during the failure phase of the geogrid. In this case, the large displacement of reinforcement will limit role of transverse members in providing the pull out capacity. Figure 2.5 depicts some results from pull out tests using feasible and rigid fronts.

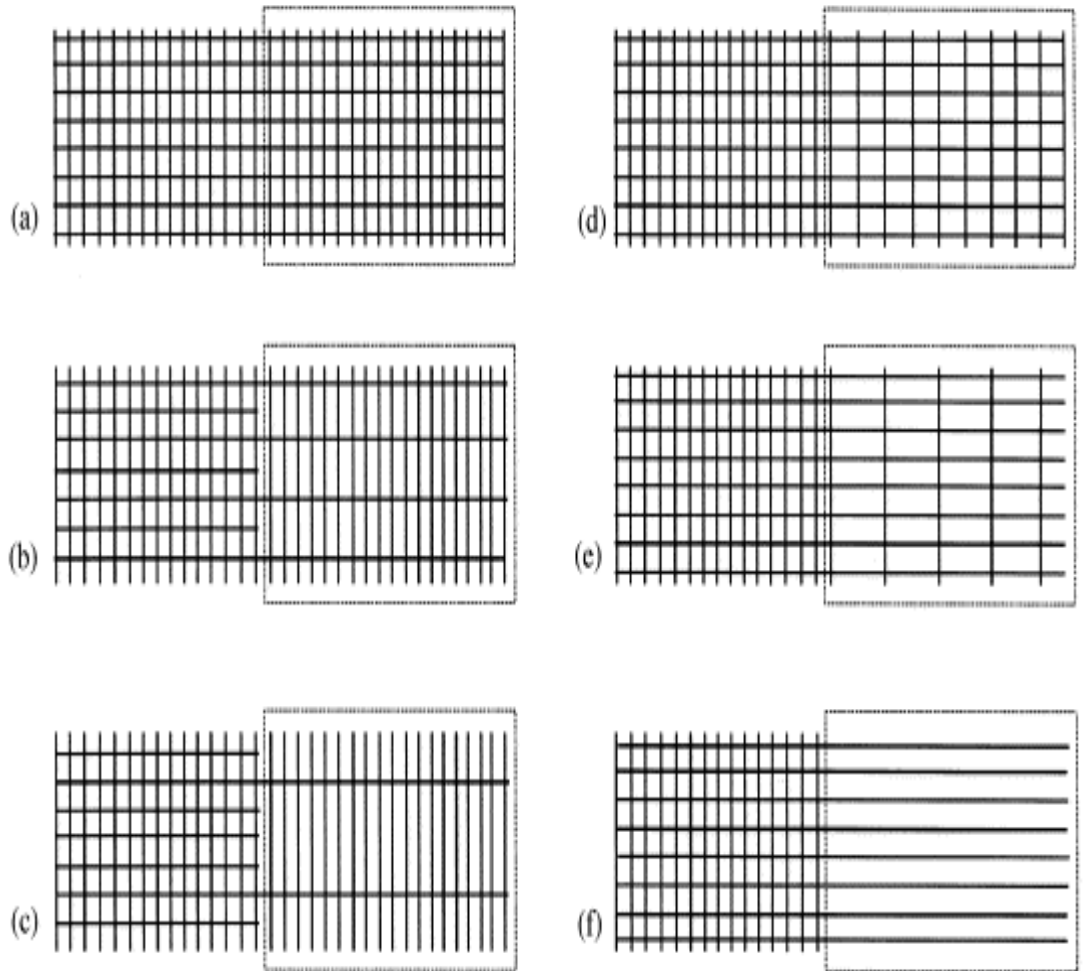


Figure 2.4: Geogrids used in pull out tests by Alagiyawanna et al., (2001)

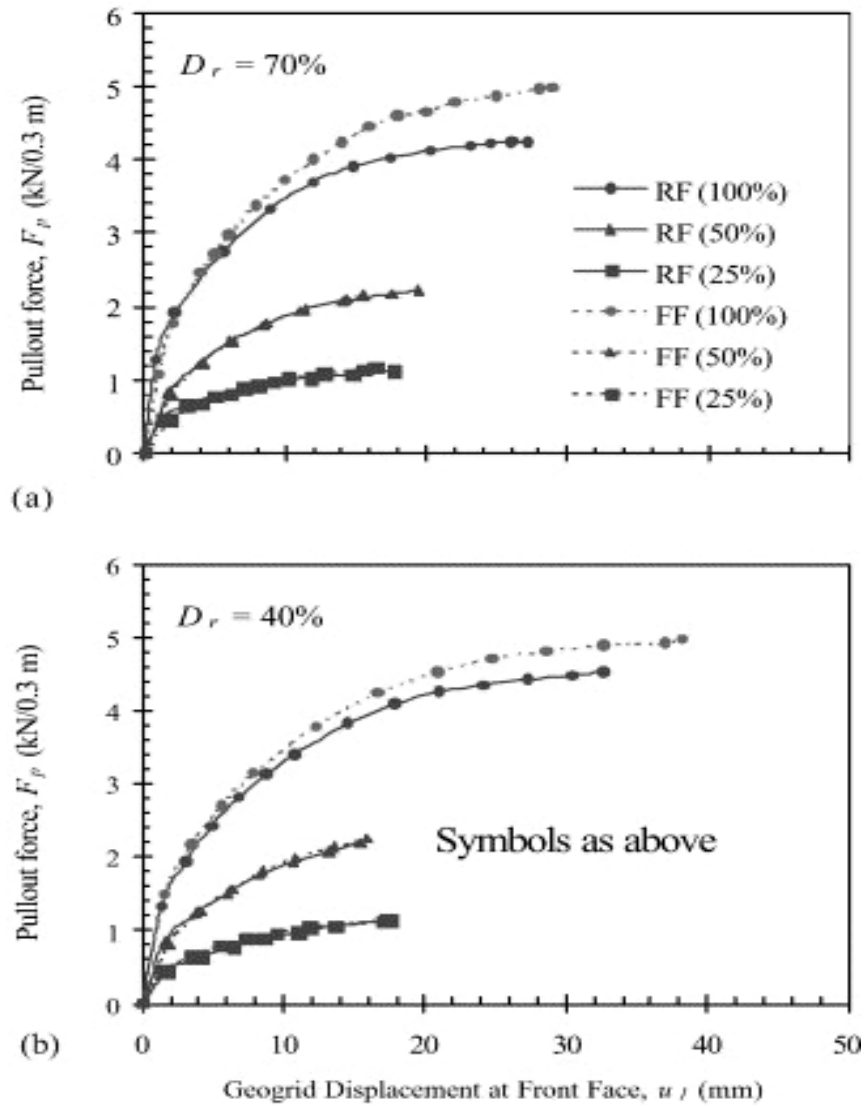


Figure 2.5: Results of pull out tests for flexible and rigid reinforcement members by Alagiyawanna et al. (2001)

Interface shear strength parameters of Geomembrane–geotextile were studied by Wasti and Bahadır Özdüzgün (2001) using 3 types of tests involving, the inclined board (tilting table), the standard sized direct shear box (60 mm×60 mm), and the large-scale direct shear box (300 mm×300 mm). HDPE, PVC geomembranes with Smooth and rough surfaces, and nonwoven needle-punched geotextiles were used in

the study. The inclined board tests were done under 5 to 50 kPa normal stresses on interface with various areas. The direct shear tests were conducted on normal stresses of 25 to 300 kPa for the smaller box and 110 to 400 kPa for the larger box. The results are given in Figure 2.6.

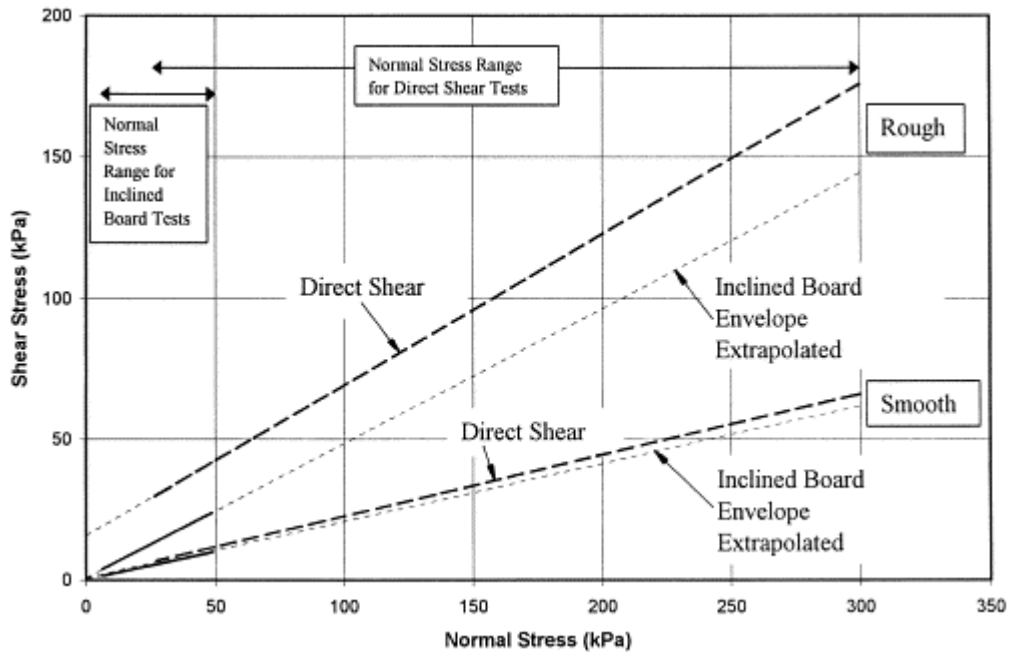


Figure 2.6: Results from inclined board test and large direct shear box tests involving 60 mm×60 mm geomembrane and geotextile interfaces (Wasti and Bahadır Özdüzgün, 2001)

The results with cohesion and interface friction angle values by fitting a straight line through the plots of interface shear strength versus the normal stresses were compared for different tests. They found that the inclined board test both smooth and rough HDPE geomembrane–geotextile interfaces had produced envelopes with small amount of adhesion. The interface size however was not significant factor. For smooth geomembranes, direct shear and inclined board tests both gave different interface friction angle and cohesion values. Their results showed

that the direct shear adhesion and friction values were markedly higher compared to those obtained from the inclined board tests, as given in table 2.1.

Table 2. 1: Different friction angle with different confining pressure (Wasti ,2001)

| Interface | Giroud et al (1990) $\bar{\sigma}=1.1$ kPa | Koubouras et al.(1991) $\bar{\sigma}=2.7$ kPa | Girard et al.(1990) $\bar{\sigma}=3.7$ kPa | Prescart study for $\bar{\sigma}=5$ or 5.5 kPa | Giroud et al (1990) $\bar{\sigma}=25-160$ kPa | Koubouras et al.(1991) $\bar{\sigma}=30-62$ kPa | Girard et al.(1990) $\bar{\sigma}=100-400$ kPa | Prescart study for $\bar{\sigma}=110-400$ kPa |
|----------------|---|--|---|---|--|--|---|--|
| Smooth HDPE-GT | — | $\delta=19$ | — | $\delta=14-21$ | | $\bar{\sigma}=2.8$ kPa $\delta=10$ | — | $\bar{\sigma}=0.7-3.3$ Kpa $\delta=12-14$ |
| Rough HDPE-GT | $\delta=45$ | $\delta=34$ | — | $\bar{\sigma}=33-42$ | $\bar{\sigma}=1.1$ Kpa $\delta=15$ | $\bar{\sigma}=17.2$ Kpa $\delta=15$ | — | $\bar{\sigma}=13-30$ Kpa $\delta=13-30$ |
| PVC-GT | — | $\delta=22$ | $\delta=25$ | $\delta=23$ | — | $\bar{\sigma}=0$ Kpa $\delta=26$ | $\bar{\sigma}=0$ Kpa $\delta=34$ | $\bar{\sigma}=1-2$ Kpa $\delta=24-25.5$ |

Goodhue et al. (2001) conducted pull out test and direct shear test to find interaction coefficient (f) between foundry sand, grids and geotextile, and textiles. Their results showed that interface friction angles had ranged from 25 to 35 degree, with efficiencies amounting to between 0.5 and 0.9. Also, the pull out tests results indicated that the interaction coefficient was varied from 0.2 to 1.7.

Racana et al. (2003), have done pull out tests on vertical, horizontal and corrugated strips of different geometries in order to validate their finite element

equations. They found that if the strain was low, more overall pull out capacity would be realized from the system. Their finite element formula also had 23% higher pull out capacity in comparison with the results from experimental study, as given in Figure 2.7 .

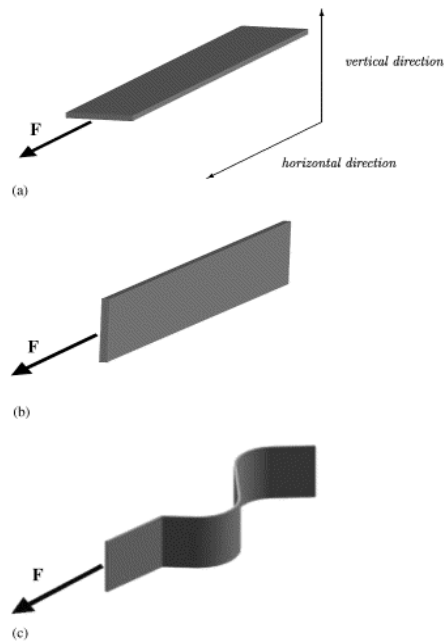


Figure 2.7: Strips of different geometries (Recana et al., 2003)

Numerical and experimental study further indicate that the low strain and overall increased pull out capacity in corrugated stripe was beneficial in the use smaller length of strips in practice as given in Figure 2.8, 2.9, and 2.10.

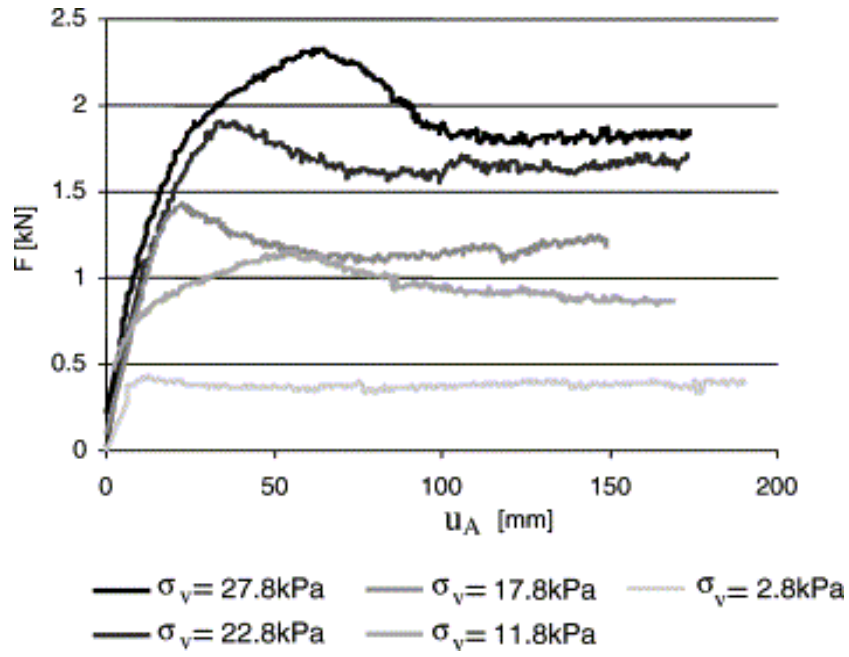


Figure 2.8: Pull out capacity for horizontal strips (Recana et al., 2003)

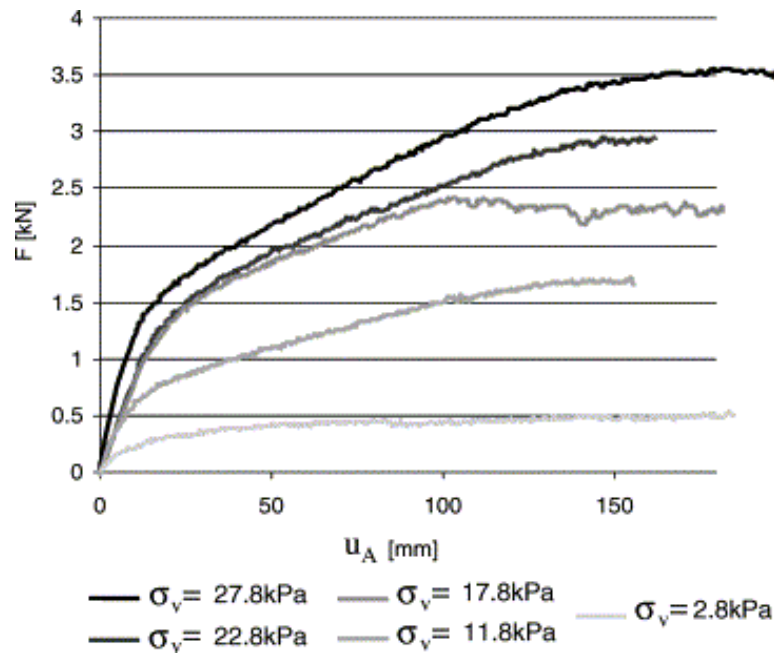


Figure 2.9: Pull out capacity for corrugated strip (Recana et al., 2003)

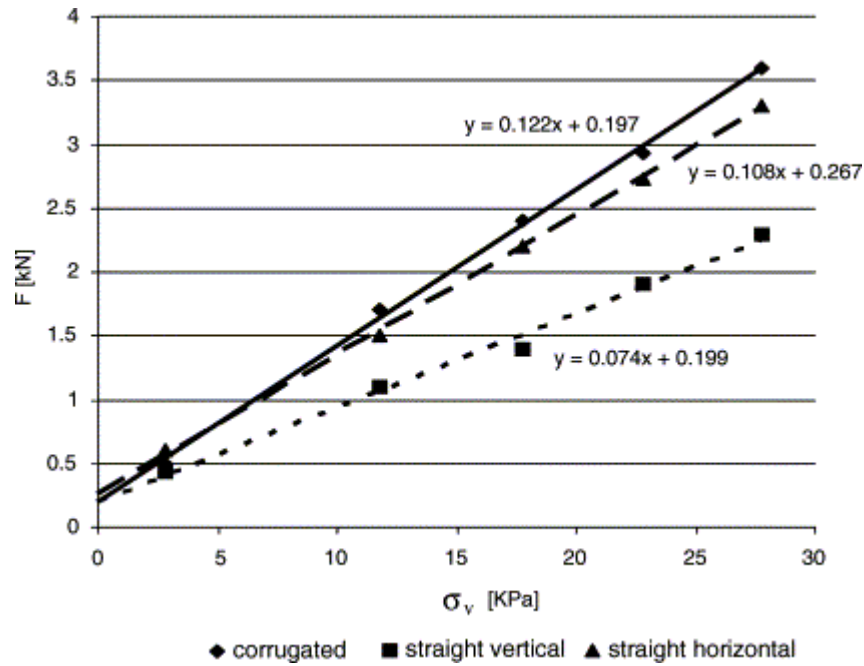


Figure 2.10: Pull out force for straight vertical, straight horizontal, and corrugated strip (Recana et al., 2003)

Palmeira (2004) studied on the mobilization of bearing forces in reinforcement during pull-out test. In this study, a theoretical model was made to describe the effects of having transverse ribs of geogrid in a large scale pull out test. Various mechanical and geometrical properties were tried with the model. Also investigated were the effects of some parameters such as free reinforcement length and test speed. He also found that good fill materials could make for shorter anchorage lengths in reinforced walls and slopes. He concluded that the length of reinforcement would affect overall stability of the reinforced mass, deformations, and final cost. Thus, the interaction between soil and geogrid is very important factor in the design of reinforce earth structure. Some results by Palmiera (2004) are given in Figure 2.11.

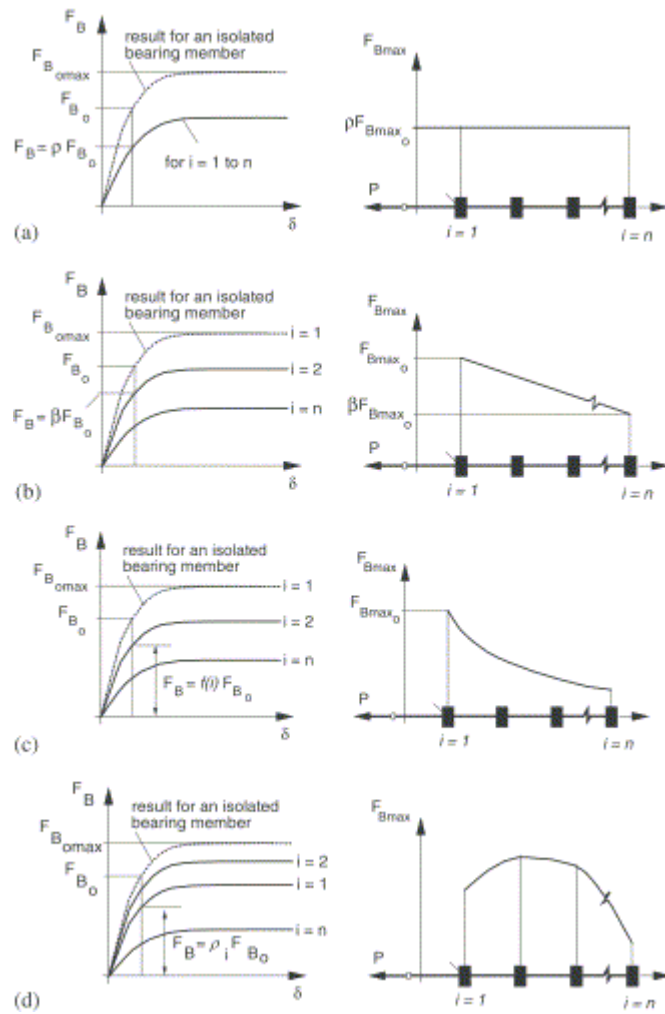


Figure 2.11: Cases of bearing strength degradation: (a) Reduction of uniform bearing force, (b) Reduction of linear bearing force along grid length, (c) reduction of bearing force as a power relation, (d) variable reduction of pull out force along the reinforcement (Palmeira, 2004)

Nejad and Smal (2005) conducted pull out test and direct shear test on geogrids and investigated interface and dilatancy angle and property in two types of soil. They have also compared the results with those coming from equations by Jewell et al. (1984) and Peterson et al. (1980). They results showed that the pull out tests showed higher amount of resistance than the direct shear tests – due to presence